



Article

The Application of JENDL-5.0 Covariance Libraries to the Keff Uncertainty Analysis of the HTTR Criticality Benchmark

Peng Hong Liem





Article

The Application of JENDL-5.0 Covariance Libraries to the Keff Uncertainty Analysis of the HTTR Criticality Benchmark

Peng Hong Liem ^{1,2}

¹ Cooperative Major in Nuclear Energy, Graduate School of Engineering, Tokyo City University (TCU), 1-28-1 Tamazutsumi, Setagaya, Tokyo 158-8557, Japan; liemph@nais.ne.jp; Tel.: +81-29-2705000; Fax: +81-29-2705001

² Scientific Computational Division, Nippon Advanced Information Service (NAIS Co., Inc.), 416 Muramatsu, Tokaimura, Naka-gun, Ibaraki 319-1112, Japan

Abstract: In this study, a 56-group covariance library was generated based on the recently released JENDL-5 covariance data, which cover 105 isotopes. The AMPX-6 code system facilitated the generation of this library. Subsequently, the TSUNAMI-IP code was employed to estimate the uncertainty in the effective neutron multiplication factor (k_{eff}) for the critical experiment conducted in the Japanese High-Temperature Test Reactor (HTTR). Our analysis involved comparing results obtained from three nuclear data libraries: JENDL-5, ENDF/B-VIII.0, and ENDF/B-VII.1. The k_{eff} uncertainty originated from the nuclear data of JENDL-5, ENDF/B-VIII.0, and ENDF/B-VII.1 and were estimated to be 0.387%, 0.581%, and 0.556%, respectively. Interestingly, when the JENDL-5 covariance library was combined with ENDF/B-VIII.0 for JENDL-5 nuclides lacking covariance data, the k_{eff} uncertainty increased to 0.464%. The primary contributors to the k_{eff} uncertainty, ranked in decreasing order, were U-235 (nubar), C-12 (n,gamma), U-235 (fission), C-12 (elastic), and U-238 (n,gamma). Notably, significant differences in the k_{eff} uncertainty were observed between JENDL-5 and ENDF/B-VIII.0, particularly for U-235 (nubar) and C-12 (elastic). Additionally, the sensitivity coefficients, similarity, and kinetics parameters were evaluated across the three libraries, leading to insightful inter-library comparison results.

Keywords: JENDL-5; covariance library; uncertainty analysis; HTTR; criticality benchmark



Academic Editor: Dan Gabriel Cacuci

Received: 16 October 2024

Revised: 18 February 2025

Accepted: 8 April 2025

Published: 23 April 2025

Citation: Liem, P.H. The Application of JENDL-5.0 Covariance Libraries to the Keff Uncertainty Analysis of the HTTR Criticality Benchmark. *J. Nucl. Eng.* **2025**, *6*, 11. <https://doi.org/10.3390/jne6020011>

Copyright: © 2025 by the author. Licensee MDPI, Basel, Switzerland. This article is an open access article distributed under the terms and conditions of the Creative Commons Attribution (CC BY) license (<https://creativecommons.org/licenses/by/4.0/>).

1. Introduction

The Japanese Evaluated Nuclear Data version 5 (JENDL-5), released in December 2021 [1], marks a significant advancement over its predecessor, JENDL-4.0, which was released in 2012 [2]. JENDL-5 was specifically developed to address critical issues related to nuclear energy development in Japan, including nuclear waste treatment and safety enhancement [3]. Notably, JENDL-5 offers an extensive neutron-induced reaction data sub-library spanning from hydrogen ($Z = 1$) to fermium ($Z = 100$) for 795 nuclides. Additionally, it includes a thermal scattering law (TSL) sub-library covering 37 materials (encompassing 62 elements). To appreciate the improvements, if one compares JENDL-5 with its predecessor, JENDL-4.0 provided neutron-induced reaction data for only 406 nuclides and a TSL sub-library for 15 materials. The expanded coverage in JENDL-5 significantly enhances the ability to evaluate the k_{eff} uncertainty due to nuclear data uncertainties. However, it is worth noting that when compared to ENDF/B-VIII.0, some nuclides and reactions still lack covariance data in the current JENDL-5 release.

In recent years, sensitivity and uncertainty (S/U) analyses have gained prominence as a critical research area. The need for high-fidelity simulations, along with quantifying

their associated uncertainties, underscores the importance of these analyses. In recent years, S/U analyses concerning new nuclear data libraries were conducted for operating research reactors and criticality assemblies [4–8]. This work covered not only commonly found uranium and mixed oxide fuel systems but also U-233 fissile-based systems. To perform S/U analysis effectively, a robust covariance library must be generated. One well-established and validated tool for this purpose is the AMPX-6 code system [9], specifically the PUFF-IV module [10]. This module plays a pivotal role in producing reliable covariance data, and facilitating accurate assessments of simulation uncertainties.

In our recent study [11], we conducted a comprehensive sensitivity and uncertainty (S/U) analysis for the Japanese High-Temperature Engineering Test Reactor (HTTR) criticality experiment. The HTTR, operated by the Japan Atomic Energy Agency (JAEA), achieved its first criticality in 1998. During the criticality experiment and HTTR commissioning, reactor physics experiments were conducted, and valuable experimental data were documented in the Handbook of the International Reactor Physics Experiment Evaluation (IRPhE) [12]. Our S/U analysis utilized the MCNP6 code [13] in conjunction with the Whisper-1.1 code [14]. We employed the ENDF/B-VII.1 nuclear data library [15], which includes a 44-group covariance library [16], for assessing uncertainties. The primary focus was on the effective multiplication factor (k_{eff}). Results from our analysis revealed that the uncertainty in the k_{eff} was determined to be 0.506%. However, despite the progress made in S/U methodologies, there remains a shortage of comprehensive covariance data. For instance, in the SCALE-6 code system [17], the ENDF/B-VII.1 and ENDF/B-VIII.0 libraries provide covariance data for 190 and 251 isotopes, respectively; however, certain nuclides and reactions still lack adequate covariance information and rely on low-fidelity (BLO) data. This study underscores the ongoing need for improved covariance data to enhance the accuracy of S/U analyses in nuclear systems.

In our present study, a covariance library was constructed based on the recently released JENDL-5 covariance data by using the same code and technique described later [18], and applied it to the sensitivity and uncertainty (S/U) analysis of the HTTR criticality benchmark. The AMPX-6 code system facilitated the generation of this covariance library. As mentioned before, JENDL-5 offers a significantly expanded set of high-quality covariance data compared to its predecessor, JENDL-4.0, so all available JENDL-5.0 covariance data were employed to enhance the accuracy of uncertainty evaluations. The sensitivity profiles and covariance data were prepared in 252 energy groups and 56 energy groups, respectively (the same neutron energy group structures of SCALE-6). Additionally, a special JENDL-5 covariance matrix was created by incorporating additional ENDF/B-VIII.0 covariance data [19] for nuclides lacking JENDL-5 covariance information. At the time the present work was initiated, it is assumed that JENDL-5.0 and ENDF/B-VIII.0 are currently at a similar state of the art, ensuring consistency between their covariance data.

Despite the availability of numerous high-fidelity critical experiments in databases such as the International Criticality Safety Benchmark Evaluation Project (ICSBEP) Handbook [20] and the International Reactor Physics Experiment Evaluation (IRPhE) Handbook [21], similarity analysis has not been conducted for the HTTR. In the present study, this gap was addressed by employing the TSUNAMI-IP module [22] to explore similarities in criticality behavior.

The present work differs from our previous work on HTTRs [11] in that the newly released JENDL-5 cross-sections and covariance data are used for the S/U analysis, and the similarity analysis is conducted for the first time. Through this study, several objectives are addressed related to the JENDL-5.0 and its application to the HTTR criticality benchmark: (1) the estimation of dominant nuclides and their associated reactions within JENDL-5.0 that significantly impact the k_{eff} , (2) quantifying the uncertainty of JENDL-5.0 with respect to

the keff and understanding its dependence on the employed covariance data, (3) providing valuable insights to contribute feedback to the JENDL evaluators and experts, facilitating further improvements in future data releases, and (4) exploring whether the criticality experiments similar to the HTTR are sufficiently available or if additional experiments are needed in the future.

The manuscript is structured as follows: First, the HTTR criticality experiments are briefly discussed. Next, the outline of the methodology employed for the sensitivity and uncertainty (S/U) analysis was given, including the use of JENDL-5.0 covariance data. Subsequently, the results of the criticality, S/U, and similarity analyses are presented and discussed. Finally, the concluding remarks on the implications of the present findings are given.

2. Description of the Japanese 30 MWth HTTR Criticality Benchmarks

The HTTR, a 30 MWth experimental reactor, employs low-enriched uranium TRISO (Tri-Structural Isotropic) fuels dispersed within a graphite matrix to form fuel pins. Graphite serves as both the moderator and reflector, while helium gas functions as the coolant. Within the International Reactor Physics Experiment Evaluation (IRPhE) Handbook, three documented HTTR benchmarks exist: (1) Start-Up Tests of the Fully Loaded Core, (2) Start-Up Tests of the Annular Core, and (3) Elevated Temperature Measurement at Zero-Power Condition. In this study, the focus is on the critical configuration of the fully loaded core during the start-up test. This configuration was intentionally designed to achieve delayed criticality, and the evaluation occurred at room temperature. Experimental data yielded a keff value of approximately 1.0025, with standard deviations (σ) of -0.0060 and $+0.0071$ [12].

Table 1 summarizes the major design parameters of HTTR. The reactor configuration includes hexagonal fuel blocks organized into 30 columns, with each column comprising five fuel blocks and two reflector blocks (located at the top and bottom). The fuel blocks are categorized into four groups based on their spatial arrangement within the core. Fuel enrichment varies among the fuel blocks, with lower enrichment positioned near the core center. Axially, the fuel enrichment also varies, resulting in higher enrichment at the top core region. Overall, the HTTR features 12 distinct types of fuel blocks, each with enrichments ranging from 3 to 10 wt.%.

Additionally, the core accommodates 15 control blocks, each housing two control rods. These control blocks are grouped as follows: (1) Group C: Located at the core center, consisting of one control block, (2) Group R1: Positioned at the second ring, comprising six control blocks, (3) Group R2: Situated at the fourth ring, containing six control blocks, and (4) Group R3: Also located at the fourth ring, consisting of three control blocks. During the critical core configuration, groups C, R1, and R2 are inserted approximately 238.5 cm into the core, while group R3 is inserted about 11 cm. Surrounding the core, the radial reflector and instrumentation blocks are adjacent to the permanent graphite reflector. Figure 1 gives an illustration of the HTTR core layout. For a comprehensive description of the core configuration and composition, readers are encouraged to consult the benchmark evaluation report in reference [12].

Table 1. Japanese 30 MWth HTTR main design parameters [11].

Power (MWth)	30
Coolant inlet/outlet temperature ($^{\circ}\text{C}$)	395/950
Primary coolant pressure (MPa)	4
Equivalent core diameter (m)	2.3
Equivalent core height (m)	2.9
Average power density (W/cm^3)	2.5

Table 1. Cont.

Power (MWth)	30
Fuel	UO ₂
U-235 enrichment (wt.%)	3 to 10
Burnup period (EFPD)	660
Fuel block (moderator)	Graphite
Coolant	He
Reflector	Graphite
Top (m)	1.16
Side (m)	0.99
Bottom (m)	1.16
Number of fuel assemblies	150
Number of fuel columns	30
Number of pairs of control rods	
In core	7
In reflector	9
Number of instrumentation columns	3

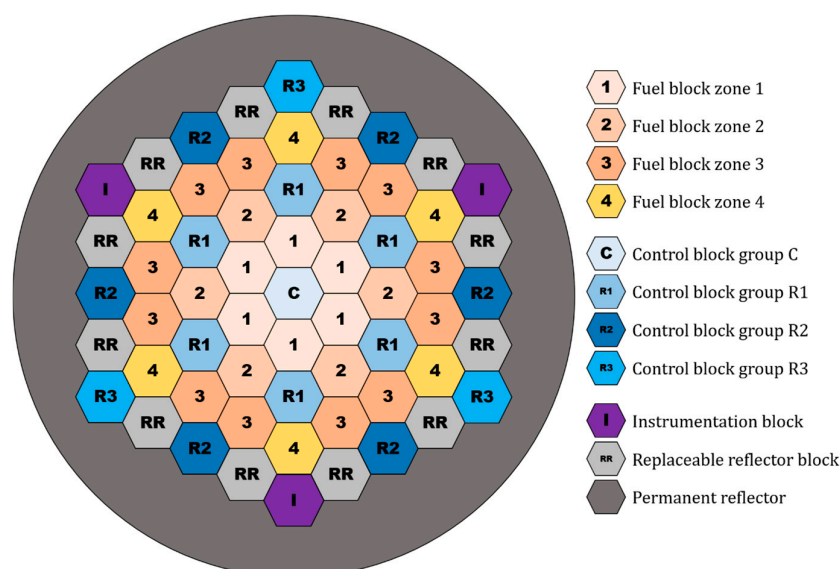


Figure 1. Radial layout of Japanese 30 MWth HTTR [11].

3. Methodology

3.1. Sensitivity, Uncertainty, and Similarity Analyses

The calculation flow for sensitivity and uncertainty (S/U) analysis, as applied to the HTTR, is similar to our previous work [18] and depicted in Figure 2. Readers may refer to the reference for a detailed discussion of the methodology. Here, the methodology is only briefly explained.

First, for the sensitivity coefficients (S_k) (252 energy groups) the MCNP6.2 code [23] with the KSEN option is employed. The KSEN option utilizes linear perturbation theory, incorporating an adjoint weighting function [24]. MCNP6.2 uses the Iterated Fission Probability (IFP) method [13,25] to compute the adjoint-weighted integrals needed for the sensitivity coefficients.

The covariance matrices ($C_{\alpha\alpha}$) in the 56 energy group COVERX format was generated using the AMPX-6 code (the PUFF-IV module). The 56 energy group structure aligns with that employed in the SCALE-6.2 [17] covariance data.

Using EXSITE and its templates, three groups of PUFF-IV-related input data were prepared: (1) point1d, (2) puff, and (3) combine_cov. In the point1d step, point-wise cross-

section data were generated, followed by Doppler broadening to a temperature of 293 K, for subsequent use in the puff process. Cross-section values were interpolated on a “super energy grid”, which is an adaptive energy mesh combining the required energy group structure and energy data points from the nuclear data file. During Doppler broadening, the default precision level (0.001) for linear interpolation was employed on the adaptive energy mesh. In the puff step, covariance matrices were generated on the calculated super energy grid from files 31 to 33, utilizing the tab1 file type, 56 energy group structure, and a weighting spectrum (core average spectrum). The weighting neutron spectrum values for collapsing to the 56 energy groups were also interpolated on the same super energy grid. Files 31 and 33 contain point-wise covariance data, while File 32 provides covariance information for resonance parameters in the resolved and unresolved energy ranges. The covariance matrices calculated on the super energy grid were then collapsed to the required 56 energy group structure by summing the contributions from each energy group. In the combine_cov step, nuclide-wise covariance matrices were merged into a single covariance library in COVERX format, which can be read by the TSUNAMI-IP module. Additionally, the same combine_cov process is used to augment the JENDL-5 with the ENDF/B-VIII.0 covariance matrices.

Amongst the 795 nuclides of JENDL-5, only 105 nuclides have covariance data [18] while ENDF/B-VIII.0 has 251 nuclides with covariance data. Given this disparity, a specialized covariance matrix for JENDL-5 was compiled by augmenting it with ENDF/B-VIII.0 covariance data for nuclides lacking their covariance information. This approach allowed comparison of the uncertainty estimates between JENDL-5 and ENDF/B-VIII.0. The ENDF/B-VIII.0 covariance data, at the time this work was conducted, were considered up to date and in the same state of the art, and were expected to fill the gap of JENDL-5. The ENDF/B-VIII.0 is relatively more complete, consistent and reliable, so it provides confidence in its accuracy when use to supplement JENDL-5. Considering the material composition of the HTTR, the covariance data of ENDF/B-VIII.0 listed in Table 2 were included. Amongst the covariance data listed in the table, Si-28, Si-29, and Si-30 are the most important since these are the main composition of the coating layers of TRISO fuel particles used in HTTR. In the future, if the calculations are extended to burned fuel then more ENDF/B-VIII.0 covariance data would be needed to fill the gap. To estimate the keff uncertainty matrix, denoted as \mathbf{U}_{kk} , one relies on sensitivity coefficients and covariance matrices. The \mathbf{U}_{kk} calculations utilize the TSUNAMI-IP module [22] from SCALE-6.3 [26]. As mentioned above, the uncertainty matrices were computed for both JENDL-5 alone and JENDL-5 combined with ENDF/B-VIII.0, using the ENDF/B-VIII.0 covariance matrices within the SCALE 6.3 framework.

For the similarity analysis, the same TSUNAMI-IP module was employed. The criticality experiments were taken from Whisper 1.1 data [14]. The similarity evaluation relies on sensitivity coefficients, either independently or in conjunction with cross-section uncertainty information. The TSUNAMI-IP’s correlation coefficient for describing the similarity is defined as

$$c_k = \frac{\sigma_{ij}^2}{(\sigma_i \sigma_j)} \quad (1)$$

where σ_{ij}^2 is the relative covariance between systems, i.e., the off-diagonal elements of relative variances matrix $\mathbf{C}_{\alpha\alpha}$.

The similarity between the HTTR core and the criticality experiments is quantified using the above-mentioned correlation factor (c_k), which ranges from 0 to 1.0. A value of (c_k) close to 1.0 indicates a strong correlation, signifying a high degree of similarity between the HTTR core and the corresponding criticality experiment.

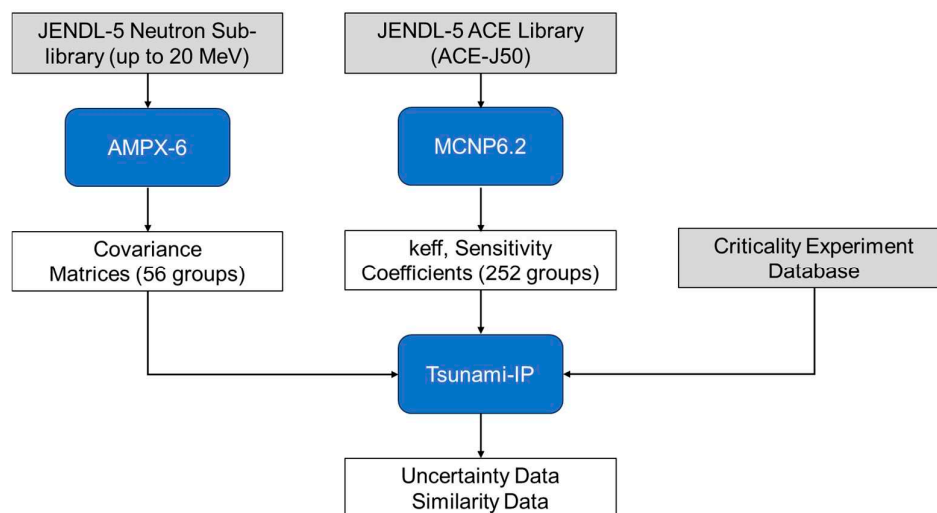


Figure 2. The calculation flow of the sensitivity, uncertainty, and similarity analysis [18].

Table 2. ENDF/B-VIII.0 covariance data included for the JENDL-5 nuclides with no covariance data.

No.	ZAID	Nuclide
1	2004	He-4
2	13,027	Al-27
3	14,028	Si-28
4	14,029	Si-29
5	14,040	Si-30
6	26,054	Fe-54
7	29,063	Cu-63
8	29,065	Cu-65

3.2. Monte Carlo Modeling

Using the MCNP6.2 code, the fully loaded HTTR core is represented in three dimensions, adhering to benchmark specifications. Within this model, TRISO particles are arranged in an ordered lattice configuration, ensuring precise fitment within the fuel pin geometry without overlap. However, it is important to note that explicit modeling of TRISO particles at random positions in MCNP6.2 presents limitations, particularly for the HTTR core, which encompasses 12 distinct fuel enrichment types. Consequently, variations in the keff value may arise due to the stochastic distribution of TRISO particles. Nevertheless, the anticipated impact on sensitivity coefficients and their associated uncertainties is expected to be negligible for the following reasons. According to the definition, the keff uncertainty is calculated based on the sensitivity coefficients and the covariance matrix. The sensitivity coefficients are not sensitive to the absolute value of the keff but to the change in the keff. Therefore, the impact on the sensitivity coefficients and the keff uncertainty would be negligible.

In our calculations using the MCNP6.2 code, based on the trade-off between computing time and statistical error, the following conditions were used: (1) Neutron histories: 10,000 per generation, (2) Generations: 1100 (including 100 inactive generations), and (3) Fractional Standard Deviation (FSD) of the keff: approximately 8 pcm. Under these conditions, the statistical errors for sensitivity and uncertainty values were adequate, especially for library comparison.

These calculations were conducted using three different nuclear data libraries: JENDL-5, ENDF/B-VIII.0, and ENDF/B-VII.1. Notably, ENDF/B-VIII.0 provides cross-section data for both C-12 and C-13, whereas ENDF/B-VII.1 includes cross-section data only for natural carbon (C natural). In the present study, the graphite material from ENDF/B-VIII.0 is defined using C-12, which constitutes approximately 98.9% of natural carbon. Additionally, the S (α,β) thermal neutron scattering library for graphite was also utilized. It is worth mentioning that ENDF/B-VIII.0 offers three distinct S (α,β) libraries for graphite, each tailored to specific porosity levels. To maintain consistency with other libraries, the S (α,β) library with 0% porosity was adopted.

For completeness, kinetics parameters were evaluated within the MCNP6.2 framework, employing the IFP method. Specifically, the adjoint angular flux required for the weighting function was defined as the asymptotic increment resulting from a progenitor neutron at a specific position, energy, and flight angle. The active cycles were split into blocks (propagation batches) to tally the adjoint-weighted kinetics parameters during the forward calculation. The default number of propagation batches, 10, was used for a converged solution in the present work.

4. Analysis Results and Discussion

4.1. Criticality Analysis

The MCNP6.2 criticality analysis results (k_{eff}) for three nuclear data libraries—JENDL-5, ENDF/B-VIII.0, and ENDF/B-VII.1—are presented in Table 3. Additionally, neutron spectra in both the core and reflector regions are depicted in Figure 3. The k_{eff} values for ENDF/B-VIII.0 and ENDF/B-VII.1 were extracted from our prior work [11]. From the Handbook of the International Reactor Physics Experiment Evaluation (IRPhE), the reported experimental k_{eff} value is 1.0025, accompanied by an uncertainty range of $-\sigma = 0.0060$ and $+\sigma = 0.0071$ (Reference [12]: Table 2.64 and Table 4.1). Notably, the document explicitly states that no biases have been evaluated to correct the expected experimental k_{eff} , except for the bias related to removing reactor instrumentation from the instrumentation columns. The uncertainty assessment meticulously accounts for both systematic and random uncertainties arising from dimensions and material compositions, including impurities.

Table 3. Criticality analysis results (k_{eff}) (pcm = 10^{-5}).

Library	k_{eff}	FSD **	[C/JENDL-5-1.0]
JENDL-5	1.01773 (1.52%)*	0.00008	-
ENDF/B-VIII.0 ***	1.02009 (1.75%)*	0.00008	+232 pcm
ENDF/B-VII.1 ***	1.01742 (1.49%)*	0.00008	−30 pcm

(*) [C/E-1.0]; Experiment data (E): $k = 1.0025$ with $-\sigma = 0.0060$ and $+\sigma = 0.0071$ (Reference [12]: Table 2.64 and Table 4.1); (**) fractional standard deviation; (***) taken from [11].

The calculated k_{eff} [C/E-1] values, as shown in Table 3, are 1.52%, 1.75%, and 1.49% for JENDL-5, ENDF/B-VIII.0, and ENDF/B-VII.1, respectively. All these values remain below 1.8%. In the same document (IRPhE), k_{eff} values obtained using older nuclear data libraries (such as ENDF/B-V.2, ENDF/B-VI.8, ENDF/B-VII.0, JEFF-3.1, and JENDL-3.3 with ENDF/B-VII.0 S (α,β)) and MCNPX (based on ENDF/B-VII.0) are also reported. These older data exhibit similar magnitudes, ranging from 1.53% to 2.10%. Despite considering experimental uncertainties, the calculated k_{eff} values based on benchmark specifications significantly deviate from the experimental k_{eff} . It is expected that future revisions of

the benchmark specifications will better reflect the actual conditions of criticality experiments [27]. As for the inter-library comparison of keff values in terms of [C/JENDL-5-1.0], the ENDF/B-VII.1 shows 30 pcm lower than JENDL-5 while the ENDF/B-VIII.0 shows a significant difference of 232 pcm higher than JENDL-5. As shown later in 4.2, amongst others, the C-12 scattering and (n, gamma) cross-sections may contribute to the keff difference since the HTTR main fuel and structural components are made of graphite.

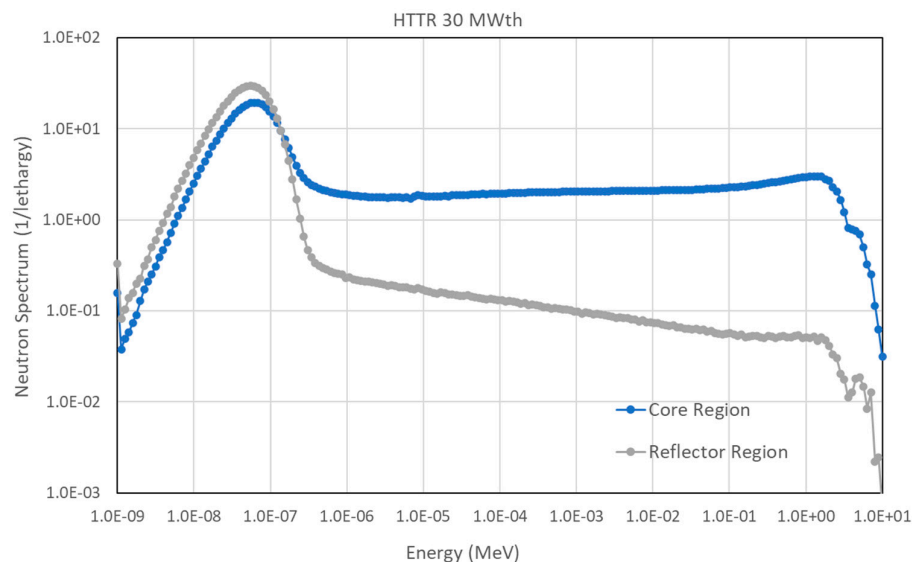


Figure 3. Neutron spectra in the core and reflector regions of the HTTR.

The JENDL-5 neutron spectra (Figure 3) show well-thermalized profiles with thermal peaks just below 0.1 eV. The neutron spectrum of the reflector region is softer than the core region and there is no fast peak in the MeV energy region.

4.2. Sensitivity Analysis

The sensitivity analyses were conducted using the KSEN option of MCNP6.2 for three nuclear data libraries: JENDL-5, ENDF/B-VIII.0, and ENDF/B-VII.1. Our focus was on obtaining sensitivity coefficients for various nuclides and nuclear reactions. These coefficients were then sorted based on their absolute magnitudes. Additionally, the sensitivity coefficients were grouped according to their signs: positive coefficients tend to increase the keff, while negative coefficients tend to decrease it. The results are presented in Tables 4 and 5. Only sensitivities with absolute values greater than 0.1% are reported. In the tables, inter-library comparison against JENDL-5 is also listed in terms of [C/JENDL-5] ratio. The underlined figures show a relative difference of more than 5%, i.e., the ratio > 1.05 or ratio < 0.95.

Table 4 highlights the dominant reactions, with elastic scattering being the most influential, followed by total nu, fission, and inelastic scattering. Notably, the present findings align with our previous work [11], where U-235 (total nu and fission) and C (elastic scattering) were among the top contributors. Similar trends were observed in the sensitivity analysis for the VHTRC [28] and HTR-PM [29]. Comparing ENDF/B-VIII.0 and ENDF/B-VII.1, significant differences in sensitivity coefficients for specific reactions were identified. Notably, C-12 (elastic), S (α,β) of C (inelastic and elastic), U-238 (elastic), and Fe-56 (elastic) exhibited relative differences exceeding 5%. These discrepancies highlight the impact of newly updated cross-sections [30] in the different libraries.

Table 4. Sensitivities of the keff in the increasing direction (abs. value > 0.1%).

Nuclide	Reaction	JENDL-5	ENDF/B-VIII.0	E80/J5 *	ENDF/B-VII.1	E71/J5 **
U-235	total nu	9.93×10^{-1}	9.93×10^{-1}	1.00	9.93×10^{-1}	1.00
U-235	fission	3.91×10^{-1}	3.90×10^{-1}	1.00	3.92×10^{-1}	1.00
C-12	elastic	2.35×10^{-1}	2.62×10^{-1}	<u>1.12</u>	2.33×10^{-1}	0.99
C (S(α,β))	inelastic	1.31×10^{-1}	9.04×10^{-2}	<u>0.69</u>	1.25×10^{-1}	0.96
C (S(α,β))	elastic	1.53×10^{-2}	2.39×10^{-2}	<u>1.56</u>	3.29×10^{-2}	<u>2.15</u>
U-238	elastic	8.94×10^{-3}	8.25×10^{-3}	<u>0.92</u>	8.23×10^{-3}	<u>0.92</u>
U-238	total nu	7.28×10^{-3}	7.33×10^{-3}	1.01	7.39×10^{-3}	1.02
U-238	fission	4.60×10^{-3}	4.65×10^{-3}	1.01	4.70×10^{-3}	1.02
Ni-58	elastic	2.05×10^{-3}	2.02×10^{-3}	0.99	2.08×10^{-3}	1.01
Fe-56	elastic	1.90×10^{-3}	2.01×10^{-3}	<u>1.06</u>	2.00×10^{-3}	1.05
C-12	inelastic	1.71×10^{-3}	1.64×10^{-3}	0.95	1.62×10^{-3}	0.95

(Underlined figures show relative differences of more than 5%) (*) E80: ENDF/B-VIII.0, J5: JENDL-5, (**) E71: ENDF/B-VII.1.

Table 5. Sensitivities of the keff in the decreasing direction (abs. value > 0.1%).

Nuclide	Reaction	JENDL-5	ENDF/B-VIII.0	E80/J5 *	ENDF/B-VII.1	E71/J5 **
U-238	n,gamma	-1.36×10^{-1}	-1.35×10^{-1}	1.00	-1.37×10^{-1}	1.01
U-235	n,gamma	-1.15×10^{-1}	-1.15×10^{-1}	1.00	-1.14×10^{-1}	0.99
C-12	n,gamma	-7.21×10^{-2}	-7.07×10^{-2}	0.98	-7.12×10^{-2}	0.99
B-10	n,alpha	-7.08×10^{-2}	-7.10×10^{-2}	1.00	-7.19×10^{-2}	1.02
Si-28	n,gamma	-2.49×10^{-3}	-2.50×10^{-3}	1.00	-2.52×10^{-3}	1.01
U-234	n,gamma	-1.29×10^{-3}	-1.32×10^{-3}	1.02	-1.34×10^{-3}	1.04

(*) E80: ENDF/B-VIII.0, J5: JENDL-5, (**) E71: ENDF/B-VII.1.

From Table 5, it is evident that negative sensitivities predominantly arise from absorption reactions, specifically (n, gamma) and (n, alpha) processes. The five major contributors in this category are U-238 and U-235 (gamma capture), Be-10 (alpha production), C (gamma capture), and Si-28 (gamma capture). The cross-sections of U-235, U-238, C, and S (α,β) of C play a crucial role in the behavior of the clean HTTR core. The present findings align with our previous work [11]. The negative sensitivity coefficients obtained from ENDF/B-VIII.0 and ENDF/B-VII.1 libraries closely resemble those from JENDL-5. However, slight differences (less than 5%) are observed in ENDF/B-VIII.0 for C and U-234 (capture), as well as in ENDF/B-VII.1 for B-10 (n, alpha) and U-234 (capture).

Additionally, energy-dependent sensitivities of the keff for major nuclide-reaction pairs are shown in Figures 4–7. These sensitivity profiles exhibit remarkable similarity to our previous work [11], and interested readers can find further details in the referenced study.

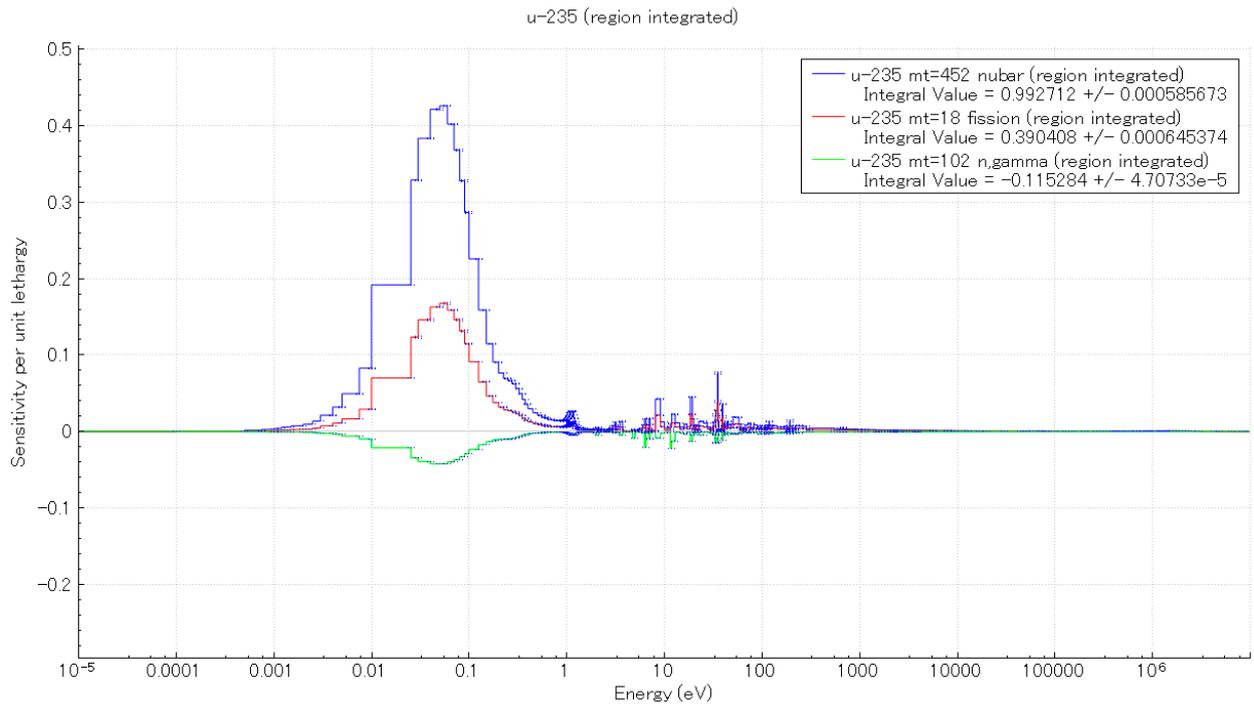


Figure 4. Energy-dependent sensitivities of the keff to U-235 cross-sections (JENDL-5).

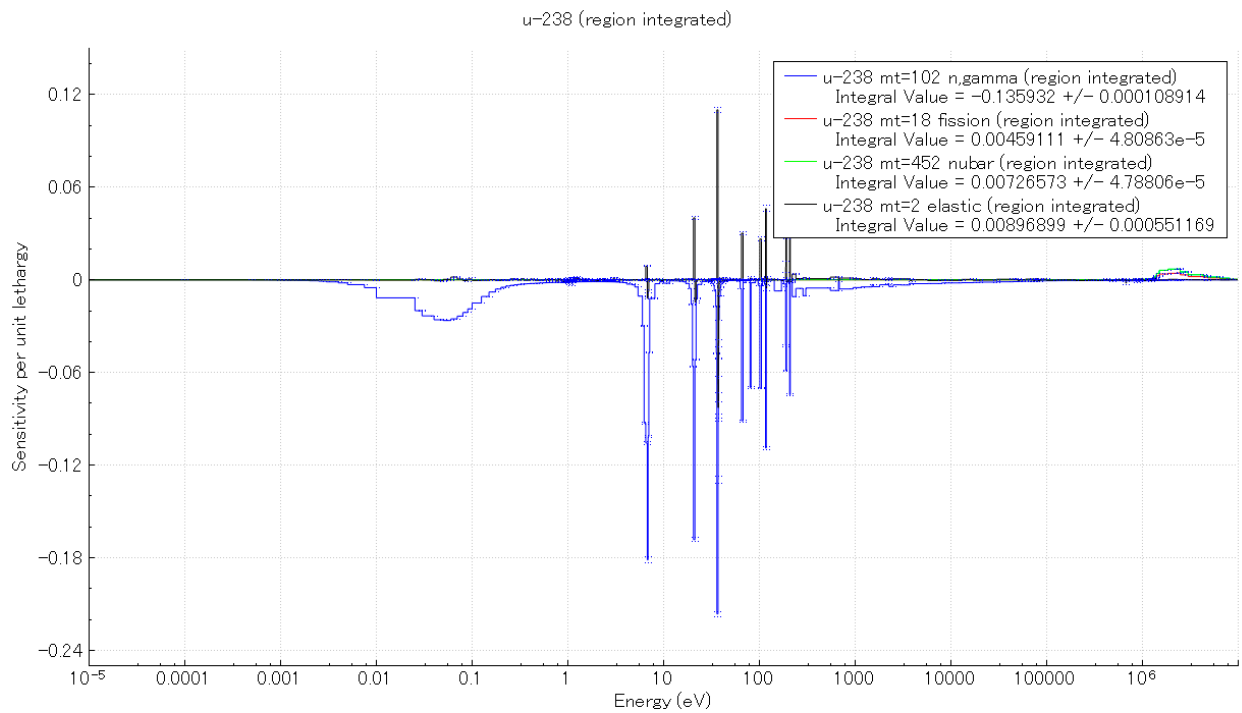


Figure 5. Energy-dependent sensitivities of the keff to U-238 cross-sections (JENDL-5).

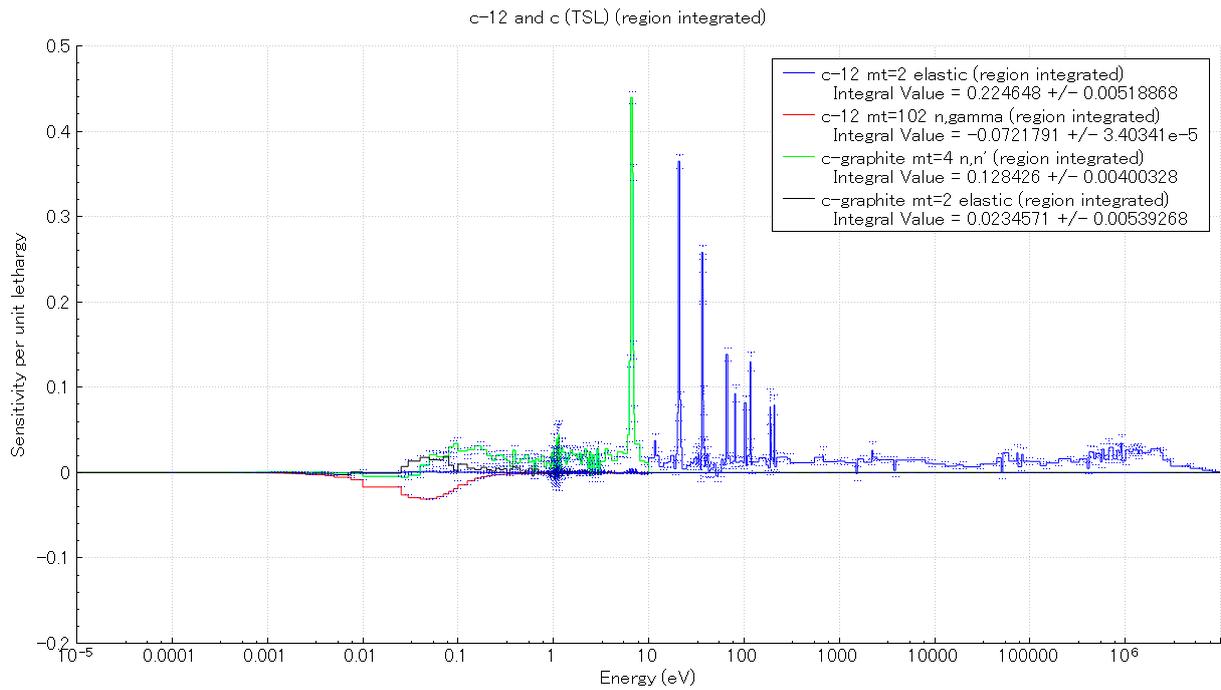


Figure 6. Energy-dependent sensitivities of the keff to C-12 and S (α,β) of C cross-sections (JENDL-5).

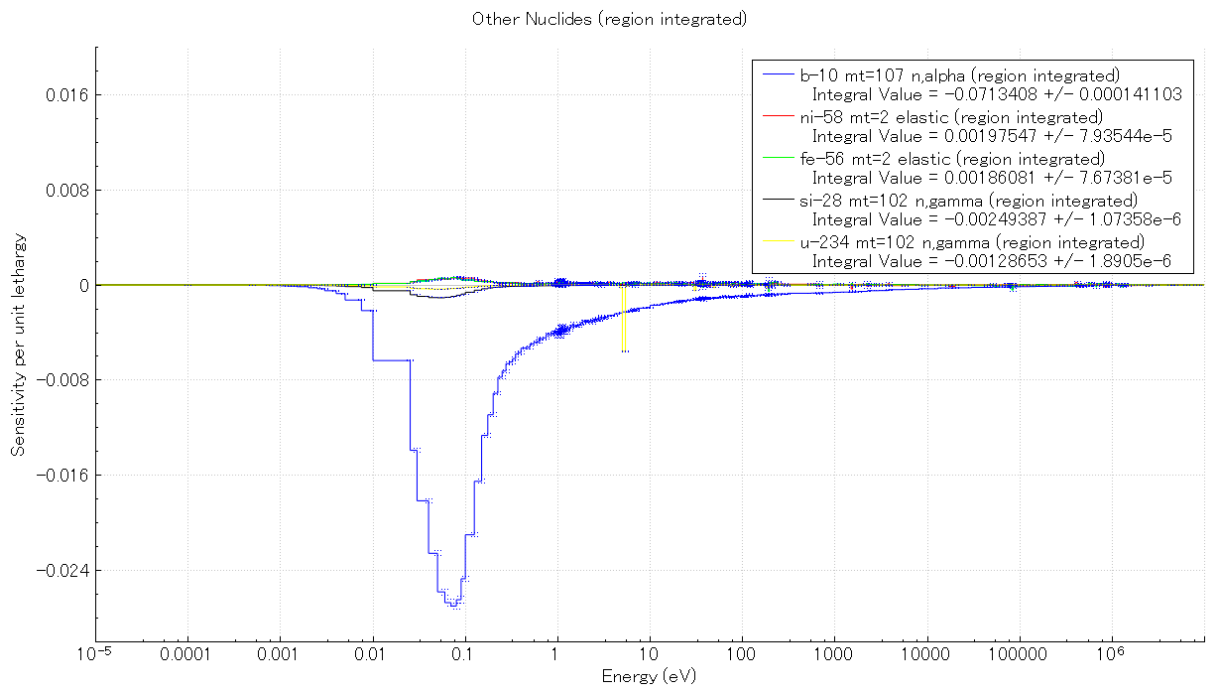


Figure 7. Energy-dependent sensitivities of the keff to B-10, Si-28, Ni-58, Fe-56, and U-234 cross-sections (JENDL-5).

4.3. Uncertainty Analysis

The keff uncertainty analysis was conducted using the TSUNAMI-IP code with three nuclear data libraries: JENDL-5, ENDF/B-VIII.0, and ENDF/B-VII.1. The results are summarized in Table 6, which presents the keff uncertainties due to nuclear data for various combinations of sensitivity coefficients and covariance matrices, and Tables 7–9, for the top contributors of each library. The table headers are reproduced directly from the code output showing the contributions of the nuclide-reaction pair taken from the original matrix form. If the nuclide-reaction pair is identical (such as U-235-fission pairing with

U-235-fission) then the dR/R is a diagonal element. The summation of the squared of dR/R elements would be equal to the uncertainty values.

Table 6. Uncertainty analysis results.

Sensitivity Coefficients	Covariance Matrices	Uncertainty (%)
JENDL-5 (MCNP6.2, KSEN option, 252 group)	JENDL-5 only (AMPX-6, 56 group)	$0.387 \pm 2.20 \times 10^{-4}$
JENDL-5 (MCNP6.2, KSEN option, 252 group)	JENDL-5 and ENDF/B-VIII.0 * (AMPX-6, 56 group)	$0.464 \pm 3.27 \times 10^{-4}$
ENDF/B-VIII.0 (MCNP6.2, KSEN option, 252 group)	ENDF/B-VIII.0 (SCALE 6.3.1, 56 group)	$0.581 \pm 2.71 \times 10^{-4}$
ENDF/B-VII.1 (MCNP6.2, KSEN option, 252 group)	ENDF/B-VII.1 (SCALE-6.2.3, 252 group)	$0.556 \pm 2.12 \times 10^{-4}$

(*) For JENDL-5 nuclides which have no covariance data.

Table 7. Uncertainty contributors (>0.001%) for JENDL-5.

Nuclide	Reaction	With Nuclide	Reaction	% dR/R Due to This Matrix		
U-235	nubar	U-235	nubar	3.00×10^{-1}	±	3.84×10^{-5}
C-12	n,gamma	C-12	n,gamma	2.16×10^{-1}	±	1.67×10^{-5}
U-235	fission	U-235	fission	1.81×10^{-1}	±	4.10×10^{-5}
C-12	elastic	C-12	elastic	1.35×10^{-1}	±	2.67×10^{-4}
U-238	n,gamma	U-238	n,gamma	1.23×10^{-1}	±	8.36×10^{-6}
U-235	chi	U-235	chi	8.64×10^{-2}	±	1.64×10^{-4}
U-238	elastic	U-238	n,gamma	3.58×10^{-2}	±	3.60×10^{-5}
B-10	n,alpha	B-10	n,alpha	3.44×10^{-2}	±	1.32×10^{-6}
U-235	n,gamma	U-235	n,gamma	3.34×10^{-2}	±	5.32×10^{-7}
U-238	elastic	U-238	elastic	2.88×10^{-2}	±	4.85×10^{-5}
U-235	fission	U-235	n,gamma	-2.77×10^{-2}	±	1.29×10^{-6}
C-12	n,n'	C-12	n,n'	1.95×10^{-2}	±	3.67×10^{-5}
U-234	n,gamma	U-234	n,gamma	1.44×10^{-2}	±	2.11×10^{-7}
C-12	elastic	C-12	n,n'	-1.04×10^{-2}	±	5.23×10^{-6}

Table 8. Uncertainty contributors (>0.001%) for ENDF/B-VIII.0.

Nuclide	Reaction	With Nuclide	Reaction	% dR/R Due to This Matrix		
U-235	nubar	U-235	nubar	4.60×10^{-1}	±	6.93×10^{-5}
C-12	n,gamma	C-12	n,gamma	2.11×10^{-1}	±	1.25×10^{-5}
U-235	fission	U-235	fission	1.81×10^{-1}	±	3.25×10^{-5}
C-12	elastic	C-12	elastic	1.64×10^{-1}	±	2.54×10^{-4}
U-238	n,gamma	U-238	n,gamma	1.23×10^{-1}	±	6.53×10^{-6}
B-10	n,alpha	B-10	n,alpha	5.51×10^{-2}	±	2.78×10^{-6}
U-238	elastic	U-238	n,gamma	3.61×10^{-2}	±	2.88×10^{-5}

Table 8. *Cont.*

Nuclide	Reaction	With Nuclide	Reaction	% dR/R Due to This Matrix		
U-235	n,gamma	U-235	n,gamma	3.36×10^{-2}	±	4.20×10^{-7}
U-238	elastic	U-238	elastic	2.90×10^{-2}	±	3.58×10^{-5}
C-12	n,n'	C-12	n,n'	1.81×10^{-2}	±	2.30×10^{-5}
U-235	fission	U-238	fission	1.48×10^{-2}	±	6.83×10^{-7}
U-235	chi	U-235	chi	1.39×10^{-2}	±	4.25×10^{-6}
U-235	fission	U-235	n,gamma	-1.04×10^{-2}	±	1.13×10^{-6}
C-12	elastic	C-12	n,n'	-1.01×10^{-2}	±	3.69×10^{-6}

Table 9. Uncertainty contributors (>0.001%) for ENDF/B-VII.1.

Nuclide	Reaction	With Nuclide	Reaction	% dR/R Due to This Matrix		
U-235	nubar	U-235	nubar	3.77×10^{-1}	±	4.32×10^{-5}
C	n,gamma	C	n,gamma	2.13×10^{-1}	±	1.16×10^{-5}
U-238	n,gamma	U-238	n,gamma	1.82×10^{-1}	±	7.74×10^{-6}
U-235	n,gamma	U-235	n,gamma	1.62×10^{-1}	±	6.45×10^{-6}
U-235	fission	U-235	fission	1.32×10^{-1}	±	1.50×10^{-5}
U-235	fission	U-235	n,gamma	1.31×10^{-1}	±	7.88×10^{-6}
C	elastic	C	elastic	1.19×10^{-1}	±	7.07×10^{-5}
U-235	chi	U-235	chi	1.02×10^{-1}	±	1.55×10^{-4}
C	n,n'	C	n,n'	3.73×10^{-2}	±	9.96×10^{-5}
U-238	elastic	U-238	n,gamma	3.62×10^{-2}	±	1.43×10^{-5}
C	elastic	C	n,n'	-3.19×10^{-2}	±	4.33×10^{-5}
U-238	elastic	U-238	elastic	2.71×10^{-2}	±	2.20×10^{-5}
C (S(α,β))	elastic	C (S(α,β))	elastic	1.41×10^{-2}	±	2.72×10^{-5}

Several covariance matrices shown in Table 6 deserve further explanation when interpreting the keff uncertainty results. The main objective of the present work is the keff uncertainty originating from the JENDL-5 nuclear data. The covariance matrix of JENDL-5 was directly processed from the JENDL-5 nuclear data. Another covariance matrix of JENDL-5 was generated by adding the covariance data of ENDF/B-VIII.0 for JENDL-5 nuclides which have no covariance data. These covariance data of ENDF/B-VIII.0 (cf. Table 2) were also processed directly from the ENDF/B-VIII.0 nuclear data. For comparison purposes, two other covariance matrices provided by the SCALE distributions were also used (56 group ENDF/B-VIII.0 and 252 group ENDF/B-VII.1) for the present uncertainty evaluations. It should be noted that these covariance matrices would differ from those directly processed from the respective nuclear data, which would produce different values of keff uncertainty.

From Table 6, one can observe the following. For the covariance library with JENDL-5 only (using only 105 covariance matrices from JENDL-5), the keff uncertainty was approximately 387 pcm. For the covariance library with JENDL-5 and ENDF/B-VIII.0 (incorporating additional covariance matrices from ENDF/B-VIII.0), the uncertainty increased to 464 pcm, resulting in a difference of approximately 77 pcm. The difference is considered to be small, and investigation revealed it was attributed to the Si isotopes. The Si isotopes are

the main composition of the fuel layers in a TRISO-coated fuel particle, i.e., they exist in a large amount in the core.

As for the SCALE covariance library with ENDF/B-VIII.0, the uncertainty was 581 pcm, surpassing that of JENDL-5. Lastly, the uncertainty for the SCALE ENDF/B-VII.1 was around 556 pcm, slightly lower than that of ENDF/B-VIII.0.

From Table 7, one can observe that the main contributors to keff uncertainty for JENDL-5 were U-235 (nubar) and (chi), C-12 (n,gamma) and (elastic), and U-238 (n, gamma). Tables 8 and 9 reveal that the top contributors to the keff uncertainty for ENDF/B-VIII.0 and ENDF/B-VII.1 were similar to those in JENDL-5. However, Table 10 highlights some key differences: As for ENDF/B-VIII.0, larger uncertainties were observed for U-235 (nubar) and C-12 (elastic) compared to JENDL-5, while for ENDF/B-VII.1, significantly larger uncertainties were found for U-235 (nubar) and U-238 (n,gamma), while U-235 (fission) and C-12 (elastic) exhibited smaller uncertainties. These variations contribute to the overall larger uncertainty in ENDF/B-VII.1 compared to JENDL-5.

Table 10. Uncertainty differences between nuclear data libraries (% dR/R, matrix diagonal elements).

Nuclide	Reaction	JENDL-5	ENDF/B-VIII.0	E80/J5 *	ENDF/B-VII.1	E71/J5 **
U-235	nubar	3.00×10^{-1}	4.60×10^{-1}	1.53	3.77×10^{-1}	1.25
C-12	n,gamma	2.16×10^{-1}	2.11×10^{-1}	0.98	2.13×10^{-1}	0.99
U-235	fission	1.81×10^{-1}	1.81×10^{-1}	1.00	1.32×10^{-1}	0.73
C-12	elastic	1.35×10^{-1}	1.64×10^{-1}	1.22	1.19×10^{-1}	0.88
U-238	n,gamma	1.23×10^{-1}	1.23×10^{-1}	1.00	1.82×10^{-1}	1.47

(*) E80: ENDF/B-VIII.0, J5: JENDL-5, (**) E71: ENDF/B-VII.1.

4.4. Similarity Analysis

The similarity analysis was conducted using the TSUNAMI-IP code to identify critical experiments closely correlated to the HTTR core. In this analysis, the JENDL-5 nuclear data library was used. The use of other nuclear data libraries is assumed to produce similar results and, therefore, is not pursued further. According to the SCALE developers' guidance, c_k of 0.9 or higher indicates a "highly similar" system while c_k between 0.8 and 0.9 is "marginally similar".

Table 11 summarizes the results for the top 20 critical benchmarks exhibiting strong correlation or similarity with the HTTR. Among these experiments, only two critical benchmarks exhibit a strong correlation coefficient ($c_k > 0.9$), namely are highly similar to the HTTR: LEU-COMP-THERM-060-005 and LEU-COMP-THERM-060-006. The LEU-COMP-THERM-060 series documents criticality experiments conducted in an RBMK graphite reactor. These experiments involve uniform configurations of UO₂ fuel assemblies, as well as configurations with empty channels, water columns, and boron or thorium absorbers, with or without water in the channels. Despite the relatively lower U-235 enrichment (<2.4 wt. %) compared to the HTTR, the benchmark series exhibit significant similarities due to their use of UO₂ fuel and graphite moderator. Other benchmark experiment series with rather strong correlation (marginally similar) to the HTTR are LEU-COMP-THERM-080 (Critical Lattices of UO₂ Fuel Rods And Perturbing Rods in Borated Water), LEU-COMP-THERM-011 (Critical Experiments Supporting Close Proximity Water Storage of Power Reactor Fuel (Part I—Absorber Rods)), LEU-COMP-THERM-017 (Water-Moderated U (2.35) O₂ Fuel Rods Reflected by Two Lead, Uranium, or Steel Walls), and LEU-COMP-THERM-005 (Critical Experiments With Low-Enriched Uranium Dioxide Fuel Rods In Water Containing Dissolved Gadolinium).

Table 11. Similarity analysis results (Top 20 with high c_k values).

No.	Benchmark Identification	c_k	Benchmark Specification
1	LEU-COMP-THERM-060-005	0.909	
2	LEU-COMP-THERM-060-006	0.905	① RBMK Graphite Reactor: Uniform Configurations of U(1.8, 2.0, or 2.4% ^{235}U)O ₂ Fuel Assemblies, and Configurations of U(2.0% ^{235}U)O ₂ Assemblies with Empty Channels, Water Columns, and Boron or Thorium Absorbers, with or without Water in Channels.
3	LEU-COMP-THERM-060-004	0.899	
4	LEU-COMP-THERM-060-003	0.895	
5	LEU-COMP-THERM-060-001	0.888	
6	LEU-COMP-THERM-060-002	0.887	
7	LEU-COMP-THERM-008-008	0.799	
8	LEU-COMP-THERM-011-007	0.798	③ Critical Experiments Supporting Close Proximity Water Storage of Power Reactor Fuel (Part I—Absorber Rods).
9	LEU-COMP-THERM-011-003	0.797	
10	LEU-COMP-THERM-008-007	0.796	
11	LEU-COMP-THERM-008-002	0.794	
12	LEU-COMP-THERM-008-005	0.794	
13	LEU-COMP-THERM-008-011	0.792	
14	LEU-COMP-THERM-011-009	0.788	
15	LEU-COMP-THERM-011-002	0.787	
16	LEU-COMP-THERM-008-001	0.783	
17	LEU-COMP-THERM-011-015	0.766	
18	LEU-COMP-THERM-017-004	0.761	④ Water-Moderated U (2.35) O ₂ Fuel Rods Reflected by Two Lead, Uranium, or Steel Walls.
19	LEU-COMP-THERM-005-004	0.753	⑤ Critical Experiments with Low-Enriched Uranium Dioxide Fuel Rods in Water Containing Dissolved Gadolinium.
20	LEU-COMP-THERM-017-006	0.751	See ④ above.

From Table 11, it can be concluded that at present there are still few criticality experiments that have a strong similarity (in this case $c_k > 0.9$) with the HTTR core. In the past, before the HTTR design and construction, JAEA (then JAERI) built Very High-Temperature Reactor Critical Assembly (VHTRC) to validate the neutronics aspect of HTTR [31]. The critical experiments of VHTRC were documented in the above-mentioned IRPhE Handbook; however, unfortunately, they were not included in the present version of Whisper 1.1 database. It is expected that a strong correlation/similarity of VHTRC to HTTR would be obtained.

4.5. Kinetics Parameter Analysis

For completeness, the kinetics parameters of the HTTR were evaluated using the JENDL-5 nuclear data library, and these results were compared with our previous assessments based on the ENDF/B-VIII.0 and ENDF/B-VII.1 libraries [11]. The comparison is summarized in Table 12. The three libraries—JENDL-5, ENDF/B-VIII.0, and ENDF/B-VII.1—yielded similar estimates for the kinetics parameters.

Table 12. Kinetics parameter evaluation results.

Nuclear Data Library	Generation Time (ms.)		Rossi-Alpha (1/ms.)		Delayed Neutron Fraction (β_{eff})	
	Value	SD *	Value	SD	Value	SD
JENDL-5	1.11843	0.00209	-5.97×10^{-3}	8.60×10^{-5}	0.00668	0.00010
ENDF/B-VIII.0	1.12404	0.00213	-5.89×10^{-3}	8.46×10^{-5}	0.00662	0.00009
ENDF/B-VII.1	1.13117	0.00213	-5.83×10^{-3}	8.31×10^{-5}	0.00659	0.00009

(*) SD: Standard deviation.

5. Concluding Remarks

Two 56-group covariance libraries were generated from the newly released JENDL-5 covariance data. The first covariance library was purely generated from the 105 isotopes' covariance data provided by JENDL-5, and the second one was generated from the JENDL-5 and ENDF/B-VIII.0 for JENDL-5 nuclides with no covariance data. Amongst the ENDF/B-VIII.0 covariance data included, the Si isotopes are the most important since they are the major composition of the TRISO fuel particles. The covariance libraries were then used for the S/U analysis of the 30 MWth fully loaded HTTR criticality benchmark, and the results were compared to ENDF/B-VIII.0 and ENDF/B-VII.1. The k_{eff} uncertainty originated from the nuclear data of JENDL-5, ENDF/B-VIII.0, and ENDF/B-VII.1 was estimated to be 0.387%, 0.581%, and 0.556%, respectively. If the JENDL-5 covariance library was combined with the ones of the ENDF/B-VIII.0 for JENDL-5 nuclides, which have no covariance data, then the k_{eff} uncertainty increased to 0.464%. The main contributors to the k_{eff} uncertainty were (in decreasing order) U-235 (nubar), C-12 (n, gamma), U-235 (fission), C-12 (elastic), and U-238 (n, gamma). Large differences in the k_{eff} uncertainty between JENDL-5 and ENDF/B-VIII.0 were found in U-235 (nubar) and C-12 (elastic). JENDL-5 lacks Si isotopes covariance data and produced slightly underestimated k_{eff} uncertainties. It is expected that in the future the covariance data for these isotopes will be available.

The similarity analysis results showed a strong correlation ($c_k > 0.9$) of LEU-COMP-THERM-060 (RBMK graphite reactor) criticality experiment series with the HTTR. Lastly, the kinetics parameters were also evaluated, and the three nuclear data libraries provided consistent results. JENDL-5's generation time, Rossi-Alpha, and effective delayed neutron fraction were evaluated to be 1.12 (ms), -5.97×10^{-3} (1/ms), and 0.00668, respectively.

It is worth mentioning that the [C/E-1] of the k_{eff} between JENDL-5, ENDF/B-VIII.0, ENDF/B-VII.1, and other nuclear data libraries, including the older version reported in the benchmark, are consistent and of a similar magnitude—about 2%. This shows that the benchmark specifications may need some improvement in the future [12,27].

Funding: This research received no external funding.

Data Availability Statement: The data presented in this study are available on request from the corresponding author.

Acknowledgments: The author acknowledges Donny Hartanto's advice and help in using AMPX-6 for generating the covariance libraries. The author expresses his gratitude to Suzuko Ikegami for the preparation of the tables and graphs.

Conflicts of Interest: The Author was employed by the company Nippon Advanced Information Service. The author declares that the research was conducted in the absence of any commercial or financial relationships that could be construed as a potential conflict of interest.

References

1. Iwamoto, O.; Iwamoto, N.; Kunieda, S.; Minato, F.; Nakayama, S.; Abe, Y.; Tsubakihara, K.; Okumura, S.; Ishizuka, C.; Yoshida, T.; et al. Japanese Evaluated Nuclear Data Library version 5: JENDL-5. *J. Nucl. Sci. Technol.* **2023**, *60*, 1–60. [[CrossRef](#)]
2. Shibata, K.; Iwamoto, O.; Nakagawa, T.; Iwamoto, N.; Ichihara, A.; Kunieda, S.; Chiba, S.; Furutaka, K.; Otuka, N.; Ohsawa, T.; et al. JENDL-4.0: A New Library for Nuclear Science and Engineering. *J. Nucl. Sci. Technol.* **2011**, *48*, 1–30. [[CrossRef](#)]
3. Iwamoto, O.; Iwamoto, N.; Shibata, K.; Ichihara, A.; Kunieda, S.; Minato, F.; Nakayama, S. Status of JENDL. In Proceedings of the 2019 International Conference on Nuclear Data for Science and Technology (ND2019), Beijing, China, 19–24 May 2019.
4. Chu, T.N.; Phan, G.T.; Bui, T.H.; Do, Q.B.; Dau, D.T.; Nguyen, K.C.; Nguyen, N.D.; Nguyen, H.T.; Hoang, V.K.; Vu, T.M.; et al. Sensitivity and uncertainty analysis of the first core of the DNRR using MCNP6 and new nuclear data libraries. *Nucl. Eng. Des.* **2024**, *419*, 112986. [[CrossRef](#)]
5. Ziani, H.; El Bardouni, T.; Lahdour, M.; El Barbari, M.; El Yaakoubi, H.; Boulaich, Y. Eigenvalue sensitivity and nuclear data uncertainty analysis for the Moroccan TRIGA Mark II research reactor using SCALE6.2 and MCNP6.2. *Nucl. Eng. Des.* **2021**, *378*, 111160. [[CrossRef](#)]
6. Aures, A.; Berner, N.; Bousquet, J.; Velkov, K.; Zwermann, W. HELIOS-2/XSUSA sensitivity and uncertainty analyses with ENDF/B-VII.1 covariance data. *Ann. Nucl. Energy* **2022**, *167*, 108857. [[CrossRef](#)]
7. Hadouachi, M.; Boukhal, H.; Chakir, E.; Belhaj, O.; Laazouzi, K.; El Yaakoubi, H.; Nouayti, A.; El Ghalbzouri, T. Nuclear data sensitivity and uncertainty analysis using a set of benchmarks containing ^{233}U comparing ENDF/B-VII.1 and ENDF/B-VIII.0 libraries. *Ann. Nucl. Energy* **2024**, *196*, 110232. [[CrossRef](#)]
8. Ahmed, A.; Boukhal, H.; El Bardouni, T.; Makhloul, M.; Chakir, E.; Ouahdani, S.E. Sensitivity and uncertainty analysis on keff due to nuclear data in the KRITZ-2:19–Comparison between JENDL-4.0 and ENDF/B-VII.1. *Ann. Nucl. Energy* **2019**, *129*, 308–315. [[CrossRef](#)]
9. Wiarda, D.; Dunn, M.E.; Greene, N.M.; Williams, M.L.; Celik, C.; Petrie, L.M. AMPX-6: A Modular Code System for Processing ENDF/B; ORNL/TM-2016/43; Oak Ridge National Laboratory: Oak Ridge, TN, USA, 2016.
10. Wiarda, D.; Dunn, M.E. PUFF-IV: A Code for Processing ENDF Uncertainty Data into Multigroup Covariance Matrices; ORNL/TM-2006/147/R1; Revised 2008; Oak Ridge National Laboratory: Oak Ridge, TN, USA, 2006.
11. Hartanto, D.; Liem, P.H. Sensitivity and Uncertainty Analyses of a High Temperature Gas-Cooled Reactor by Using a 44-Group Covariance Library. *Ann. Nucl. Energy* **2021**, *151*, 107943. [[CrossRef](#)]
12. Bess, J.D.; Fujimoto, N. Evaluation of the Start-up Core Physics Tests at Japan’s High Temperature Engineering Test Reactor (Fully-loaded Core), HTTR-GCRRESR-001, Rev. 1. In *International Handbook of Evaluated Reactor Physics Benchmark Experiments*; NEA/NSC/DOC(2006)1; Organisation for Economic Co-Operation and Development/Nuclear Energy Agency: Paris, France, 2010.
13. Kiedrowski, B.C. *Theory, Interface, Verification, Validation, and Performance of the Adjoint-Weighted Point Reactor Kinetics Parameter Calculations in MCNP*; LA-UR-10-01700; Los Alamos National Laboratory: Los Alamos, NM, USA, 2010.
14. Kiedrowski, B.C.; Brown, F.B.; Conlin, J.L.; Favorite, J.A.; Kahler, A.C.; Kersting, A.R.; Parsons, D.K.; Walker, J.L. Whisper: Sensitivity/Uncertainty-Based Computational Methods and Software for Determining Baseline Upper Subcritical Limits. *Nucl. Sci. Eng.* **2015**, *181*, 17–47. [[CrossRef](#)]
15. Chadwick, M.B.; Herman, M.; Obložinský, P.; Dunn, M.E.; Danon, Y.; Kahler, A.C.; Smith, D.L.; Pritychenko, B.; Arbanas, G.; Arcilla, R.; et al. ENDF/B-VII.1 Nuclear Data for Science and Technology: Cross-Sections, Covariances, Fission Product Yields and Decay Data. *Nucl. Data Sheets* **2011**, *112*, 2887–2996. [[CrossRef](#)]
16. Brown, F.B.; Rising, M.E. *Covariance Data File Formats for Whisper-1.0 & Whisper-1.1*; LA-UR-17-20098; Los Alamos National Laboratory: Los Alamos, NM, USA, 2017.
17. Rearden, B.T.; Jessee, M.A. (Eds.) *SCALE Code System*; ORNL/TM-2005/39 Version 6.2.1; Oak Ridge National Lab. (ORNL): Oak Ridge, TN, USA, 2016.
18. Liem, P.H.; Hartanto, D. JENDL-5 Nuclear Data Sensitivity, Uncertainty, and Similarity Analyses on the Criticality of RSG GAS Multipurpose Research Reactor. *Nucl. Eng. Des.* **2024**, *418*, 112899. [[CrossRef](#)]
19. Bostelmann, R.; Holcomb, A.; Wiarda, D.; Wieselquist, W. On the creation of the new ENDF/B-VIII.0 Covariance Library for SCALE Applications with AMPX. In Proceedings of the International Conference on Mathematics and Computational Methods Applied to Nuclear Science and Engineering (M&C 2021), Raleigh, NC, USA, 3–7 October 2021.
20. OECD/NEA. *International Handbook of Evaluated Criticality Safety Benchmark Experiments*; OECD Nuclear Energy Agency: Paris, France, 2016.
21. OECD/NEA. *International Handbook of Evaluated Reactor Physics Benchmark Experiments*; OECD Nuclear Energy Agency: Paris, France, 2017.
22. Rearden, B.T.; Jessee, M.A. (Eds.) *Tsunami Utility Modules*; ORNL/TM-2005/39 Version 6, Vol. III, Sect M18; Oak Ridge National Lab. (ORNL): Oak Ridge, TN, USA, 2009.

23. Armstrong, J.; Brown, F.B.; Bull, J.S.; Casswell, L.; Cox, L.J. *MCNP User's Manual*; Code Version 6.2, LA-UR-1729981; Werner, C.J., Ed.; Oak Ridge National Lab. (ORNL): Oak Ridge, TN, USA, 2017.
24. Kiedrowski, B.C.; Brown, F.B. Adjoint-Based k -Eigenvalue Sensitivity Coefficients to Nuclear Data Using Continuous-Energy Monte Carlo. *Nucl. Sci. Eng.* **2013**, *174*, 227–244. [[CrossRef](#)]
25. Kiedrowski, B.C.; Brown, F.B. Adjoint-Weighted Kinetics Parameters with Continuous Energy Monte Carlo. *Trans. Am. Nucl. Soc.* **2009**, *100*, 297–299.
26. Wieselquist, W.A.; Lefebvre, R.A. (Eds.) *SCALE 6.3.0 User Manual*; ORNL/TM-SCALE-6.3.0; Oak Ridge National Lab. (ORNL): Oak Ridge, TN, USA, 2021.
27. Bess, J.D.; Fujimoto, N. Benchmark Evaluation of Start-Up and Zero-Power Measurements at the High-Temperature Engineering Test Reactor. *Nucl. Sci. Eng.* **2014**, *178*, 414–427. [[CrossRef](#)]
28. Strydom, G.; Bostelmann, F. *Nuclear Data Uncertainty and Sensitivity Analysis of the VHTRC Benchmark Using SCALE*; INL/JOU-17-42606-Revision-0; Idaho National Laboratory: Idaho Falls, ID, USA, 2017.
29. Wu, Y.; Wang, L.; Wang, Y.; Guo, J.; Li, F. Sensitivity Analysis of Initial Critical State Modeling with VSOP Code. In Proceedings of the PHYSOR 2018, Cancun, Mexico, 22–26 April 2018.
30. Brown, D.A.; Chadwick, M.B.; Capote, R.; Kahler, A.C.; Trkov, A.; Herman, M.W.; Sonzogni, A.A.; Danon, Y.; Carlson, A.D.; Dunn, M.; et al. ENDF/B-VIII.0: The 8-th Major Release of the nuclear reaction data library with CIELO-Project Cross Sections, New Standards and Thermal Scattering Data. *Nucl. Data Sheets* **2018**, *148*, 1–42. [[CrossRef](#)]
31. Yasuda, H.; Akino, F.; Yamane, T.; Yoshihara, F.; Kitadate, K.; Yoshifuji, H.; Takeuchi, M.; Ono, T.; Kaneko, Y. *Construction of VHTRC (Very High Temperature Reactor Critical Assembly)*; JAERI-1305; Japan Atomic Energy Research Inst: Tokai, Japan, 1987.

Disclaimer/Publisher's Note: The statements, opinions and data contained in all publications are solely those of the individual author(s) and contributor(s) and not of MDPI and/or the editor(s). MDPI and/or the editor(s) disclaim responsibility for any injury to people or property resulting from any ideas, methods, instructions or products referred to in the content.